Demonstrating the self-healing behaviour of some selected ceramics under combustion chamber conditions

Farle, A.; Boatemaa, L.; Shen, L.; Gövert, S.; Kok, J. B W; Bosch, M; Yoshioka, S.; Van Der Zwaag, S.; Sloof, W. G.

DOI
10.1088/0964-1726/25/8/084019

Publication date
2016

Document Version
Final published version

Published in
Smart Materials and Structures

Demonstrating the self-healing behaviour of some selected ceramics under combustion chamber conditions

OPEN ACCESS
IOP Publishing
Smart Materials and Structures
Smart Mater. Struct. **25** (2016) 084019 (10pp)
doi:10.1088/0964-1726/25/8/084019

Demonstrating the self-healing behaviour of some selected ceramics under combustion chamber conditions

A Farle[1], L Boatemaa[1], L Shen[1], S Gövert[2], J B W Kok[2], M Bosch[1], S Yoshioka[3], S van der Zwaag[4] and W G Sloof[1]

[1] Department of Materials Science and Engineering, Delft University of Technology, Mekelweg 2, 2628CD, Delft, The Netherlands
[2] University of Twente, Laboratory of Thermal Engineering, PO Box 217, 7500 AE Enschede, The Netherlands
[3] Graduate School of Engineering, Yokohama National University, 79-5, Tokiwadai, Hodogaya-ku, Yokohama, Japan
[4] Faculty of Aerospace Engineering, Delft University of Technology, Kluyerweg 1, 2629HS, Delft, The Netherlands

E-mail: A.M.Farle@TuDelft.nl

Received 23 February 2016, revised 6 June 2016
Accepted for publication 29 June 2016
Published 15 July 2016

Abstract

Closure of surface cracks by self-healing of conventional and MAX phase ceramics under realistic turbulent combustion chamber conditions is presented. Three ceramics namely; Al_2O_3, Ti_2AlC and Cr_2AlC are investigated. Healing was achieved in Al_2O_3 by even dispersion of TiC particles throughout the matrix as the MAX phases, Ti_2AlC and Cr_2AlC exhibit intrinsic self-healing. Fully dense samples (>95%) were sintered by spark plasma sintering and damage was introduced by indentation, quenching and low perpendicular velocity impact methods. The samples were exposed to the oxidizing atmosphere in the post flame zone of a turbulent flame in a combustion chamber to heal at temperatures of approx. 1000 °C at low pO_2 levels for 4 h. Full crack-gap closure was observed for cracks up to 20 mm in length and more than 10 μm in width. The reaction products (healing agents) were analysed by scanning electron microscope, x-ray microanalysis and XRD. A semi-quantification of the healing showed that cracks in Al_2O_3/TiC composite (width 1 μm and length 100 μm) were fully filled with TiO_2. In Ti_2AlC large cracks were fully filled with a mixture of TiO_2 and Al_2O_3. And in the Cr_2AlC, cracks of up to 1.0 μm in width and more than 100 μm in length were also completely filled with Al_2O_3.

Keywords: combustion environment, ceramics, MAX-phase ceramics, self-healing

(Some figures may appear in colour only in the online journal)

1. Introduction

In recent years the possibility to oxidatively heal surface cracks in high temperature ceramics and metallo-ceramics and to restore mechanical strength at least once has been demonstrated in quite a number of laboratory studies [1–3]. In these laboratory studies relatively high oxygen potentials (comparable to those in heated air) and stagnant air were imposed and the samples were not exposed to any mechanical vibration during the healing treatment. These conditions differ significantly from the prevailing conditions (low partial pressure, very high gas flow velocities and extensive mechanical vibrations) in combustion chambers, where such self-healing ceramics are supposed to be used [4]. The work presented here describes the self-healing behaviour of three

grades of self-healing ceramics under realistic combustion chamber conditions. The materials to be tested are an extrinsic self-healing system (alumina containing TiC particles as healing agent) and two intrinsic self-healing metallo-ceramics (Cr_2AlC and Ti_2AlC), for which attractive self-healing behaviour under laboratory conditions had been demonstrated previously.

The early research on self-healing high temperature ceramics focussed on so-called *extrinsic* self-healing concepts, in which the crack filling reaction is due to the presences of discrete reactive particles homogeneously distributed in an inert ceramic matrix [4–6]. When a crack is formed in the matrix, the reactive particles in the path of the crack are dissected and oxygen from the environment flowing through the crack can react with the healing particle. In case the reaction product has a larger specific volume than the original particle the excess volume can fill the crack and restore mechanical contact between both opposing crack faces. In case the reaction product adheres relatively well to the matrix material, the filling of the crack not only leads to its sealing but also to the restoration of the tensile strength of the once broken sample. The early work focused on the use of SiC particles or fibres to heal Si_3N_4, mullite and alumina matrices [5, 7, 8] as SiC has a desirable oxidation behaviour leading to the formation of SiO_2 which has a good bond strength to many ceramic matrices. By using SiC particles with a size of about 0.3 μm the bending strength of Si_3N_4/SiC composites could be recovered more or less completely by healing between 900 °C and 1400 °C for 1 h in air. For the optimum healing temperature of 1300 °C the specimen fractured even outside the healed zone [5]. Similarly, surface cracks of diameter 100–200 μm in mullite were completely healed after heat treatment at 1300 °C for 1 h in air. The crack-healed zone even had a bending strength 150 ± 30 MPa higher than that of the as received material [7].

The optimal volume fraction of granular healing particles was found to be between 15% and 30% [9–11]. In recent work it has been shown that SiC whiskers rather than granular SiC particles can improve the healing capabilities even further [8] and restore not only strength but also fracture toughness. It was shown that surface cracks with a length of 100 μm could be healed in a composite containing 20 vol% of 30–100 μm long SiC whiskers. The fracture toughness increased from 3 to 4 Mpa $m^{1/2}$ for monolithic alumina to 5.6 Mpa $m^{1/2}$, and it was reported that the average bending strength after healing is 970 MPa as compared to 1000 MPa for the virginal material. Since then, systematic studies have been done on the effect of crack healing conditions on the mechanical behaviour of the crack healed zone [4, 12] the maximum crack size which can completely be healed [13] and the crack healing behaviour under static or cyclic loading and crack healing potential [5, 14].

While SiC additions work rather well, the temperature to induce optimal healing is rather high (1300 °C) and there is a need for lower healing temperatures. TiC has recently been identified and an attractive alternative [15]. The potential of TiC in healing alumina was assessed based on detailed theoretical analysis of the healing reaction and the intrinsic properties of the reaction products TiO_2 (rutile). A systematic analysis of its thermodynamic stability, relative volume expansion, work of adhesion between the healing agent and the matrix, and a comparison of the coefficient of thermal expansion between the matrix and the healing oxide revealed TiC is indeed a potentially attractive healing particle for extrinsic self-healing ceramic systems. Experimentally this was proven when surface cracks of length 100 μm in Al_2O_3–TiC composites containing 30 vol% TiC particles showed complete tensile strength recovery by annealing for 1 h at 800 °C in air.

The alternative approach to *extrinsic* self-healing systems in which the healing reaction is due to the intentional addition of a sacrificial phase is that of *intrinsic* self-healing systems in which the material itself can locally undergo healing reactions. In 2008 metallo-ceramic MAX phases, in particular Ti_3AlC_2, were shown to demonstrate significant self-healing when exposed to high temperatures in oxygen containing atmospheres [16, 17]. The underlying mechanism in the healing reaction is the selective oxidation of the A element in the MAX phases, such as Ti_3AlC_2 and Ti_2AlC as well as Cr_2AlC [16, 18, 19]. Cracks in Ti_2AlC MAX phase ceramics of up to some millimetres in length and about 5 μm in width can be healed by oxidation at 1100 °C in air within 2 h [17, 20] leading to full strength recovery. Also cracks running along the same path as previously healed cracks can be restored several times [17]. The healing is due to the extensive formation of Al_2O_3 in the crack with minor amounts of the weaker TiO_2 phase. Cr_2AlC MAX phase also shows good self-healing behaviour but the reaction rates are a bit slower. Yet the guaranteed absence of the weak TiO_2 in the healed cracks may lead to higher strength values for the healed material [21]. Hence Ti_2AlC and Cr_2AlC were selected for testing under combustion chamber conditions as both materials meet all requirements postulated for successful healing of crack damage [22], e.g. preferential oxidation and fast diffusion of the A-element, volume expansion upon oxidation and adhesion of the healing product to the matrix. As earlier studies [19, 23] on the MAX phase materials have shown that the healing kinetics and the mode of filling of the cracks depends on the grain size, Cr_2AlC samples were produced having two different average grain sizes. The influence of commonly present impurities, such as TiC and Ti_xAl_y in Ti_2AlC are considered by producing MAX phases of different purity grades.

Apart from their self-healing potential MAX phases have interesting mechanical and physical properties, which make them interesting materials for combustion chambers: They are stable up to high temperatures and corrosion resistant [1–3, 24]. Their high thermal conductivity makes them thermal shock resistant [25] and their static strength is maintained up to high temperatures, above which creep will become the limiting factor [26, 27].

In the present work we will demonstrate the self-healing behaviour of three promising self-healing ceramics (alumina

Table 1. Starting powders for synthesis and sintering.

Powder	Purity (%)	Particle size (μm)	Supplier
Al_2O_3	⩾99.99	0.2	Sumitomo Chemicals, Japan
TiC	98	4.5	Alfa Easer, UK
Ti	>99.5	100	TLS Technik GmbH & Co., Germany
Al	99.8	45	TLS Technik GmbH & Co., Germany
Cr	99.2	100	TLS Technik GmbH & Co., Germany
C (Graphite)	>99.5	6	Graphit Kropfmühl AG, Germany

Table 2. Powder composition and sintering conditions for preparing the self-healing ceramics.

Sample	Powder			Ratio	Temperature (°C)	Pressure (MPa)	Duration (min)
Al_2O_3/TiC	Al_2O_3	TiC		0.8:0.2 mass % Al_2O_3:TiC	1500	30	10
Ti_2AlC-P	Ti	Al	TiC	0.85:1.05:1.15	1400	50	30
Ti_2AlC-LP	Ti	Al	TiC	0.85:1.05:1.15	1400	50	60
Cr_2AlC_FG	Cr	Al	C	2:1.15:1	1250	50	60
Cr_2AlC_CG							

with TiC as healing agent, phase pure and impure Ti_2AlC and fine and coarse grained Cr_2AlC) under real combustion chamber conditions. First the synthesis of these ceramics will be outlined. Then their microstructure and oxidation behaviour will be discussed. Next, different methods to create crack damage are presented. Finally, the results of testing the self-healing ceramics with crack damage under real combustion conditions are evaluated.

2. Materials and methods

2.1. Synthesis

Discs of the self-healing ceramics Al_2O_3/TiC, Ti_2AlC and Cr_2AlC with a diameter of 20 mm and a thickness of about 5 mm were prepared by spark plasma sintering (SPS). The powders used to sinter the materials are listed in table 1. These powders were mixed with molar ratios specified in table 2 using a Turbula T2C Mixer (Willy A Bachofen, Switzerland), for 24–48 h using 5 mm alumina balls. The ball to powder weight ratio was about 3:1. The powder mixtures for Ti_2AlC and Al_2O_3/TiC were sintered directly in the SPS furnace (HP D 25 SD, FCT Systeme GmbH, Germany) using a graphite mould with an inner diameter of 20 mm under Argon atmosphere or in vacuum.

The Al_2O_3/TiC composite was sintered at 1500 °C in Ar and cooled naturally to avoid cracking due to thermal shock. Ti_2AlC samples were directly synthesised by SPS using the settings specified in table 2 and a heating rate of 80 °C min^{-1}. The experiments were performed in vacuum. Cr_2AlC was prepared by a two-step sintering process described elsewhere [28]. The coarse grained material was densified directly from pulverized pressureless sintered powder and fine grained sample was sintered from ball milled powders, details can be found in table 2.

Finally the surfaces of the sample were ground using emery paper up to grit 4000, ultrasonically cleaned in ethanol and dried by blowing with pure and dry nitrogen gas.

2.2. Characterisation

The density of the sintered materials was measured with the Archimedes method using an analytical balance (Mettler Toledo AG-204, Switzerland) according to ASTM B 311-93 [29]. The Vickers hardness was determined by averaging the results from 10 to 50 N indents using a hardness tester (Zwick/Z2.5, Germany). The indents were created by loading the indenter with 5 N s^{-1} and a holding time of 20 s.

The Al_2O_3/TiC composite was characterised using the x-ray diffractometer with a Lynxeye position sensitive detector and Cu Kα radiation. The phase purity of the MAX-phase samples was determined via x-ray diffraction using a Bruker D8 Advance diffractometer (Bruker, Germany) in the Bragg–Brentano geometry with graphite monochromator and Co and Cu Kα radiation. The recorded x-ray diffractrograms were processed with Bruker software Diffrac.EVA 4.1 software.

Microstructure, crack morphology and crack filling were investigated using a scanning electron microscope (SEM), type JSM 6500F (JEOL Ltd, Tokyo, Japan) equipped with an energy dispersive spectrometer (EDS, type: ThermoFisher UltraDry 30 mm^2 detector) for x-ray microanalysis (XMA) and with Noran System Seven software package for data acquisition and analysis.

The oxidation kinetics of powders of the healing materials (TiC, Ti_2AlC and Cr_2AlC) were investigated with combined thermogravimetry and differential thermal analysis (TGA/DTA) using a SETSYS Evolution 1750 (Setaram, France). To this end 20 ± 1 mg powder is put into 250 μl alumina crucible and heated to 1400 °C at different heating rates (1, 2, 5, 10 and 15 °C min^{-1}) in a flow of pure and dry synthetic air, i.e. 40 ml min^{-1} of N_2 (>5 N) and 10 ml min^{-1} of O_2 (>5 N). The relation between the heating rate β and the

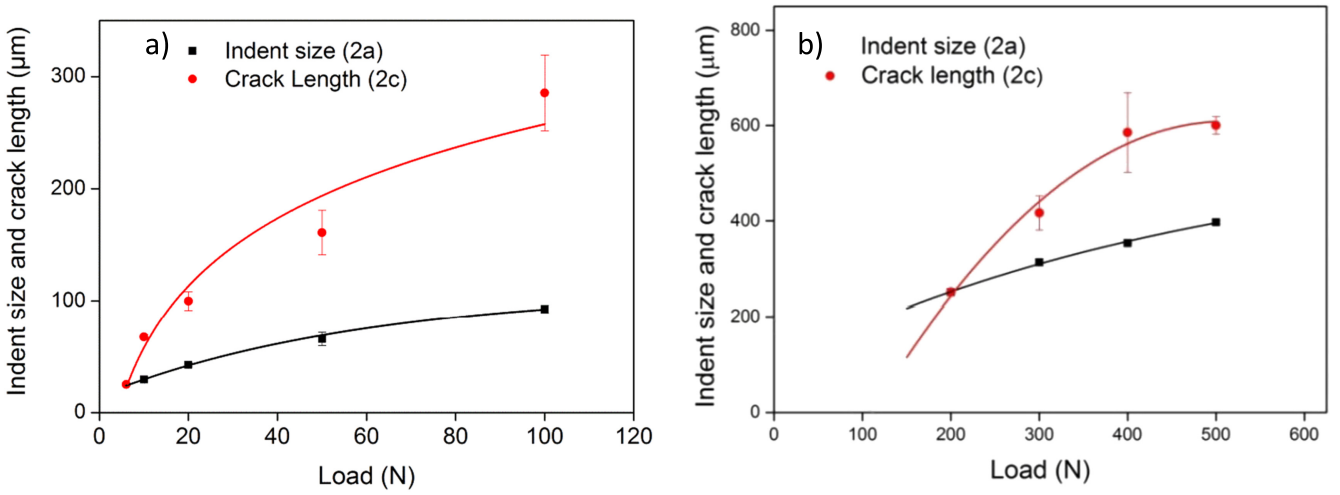

Figure 1. Vickers Indent size and crack length versus applied load of (a) Al_2O_3 with 20 vol% TiC composite and (b) fine grained Cr_2AlC.

measured peak temperature (T_p) is given by the Kissinger–Sunose–Akahira equation [30]:

$$\ln\left(\frac{\beta}{T_P^2}\right) + \frac{E_A}{RT_p} = \text{constant}, \quad (1)$$

where E_A is the activation energy and R is the gas constant. The slope of a straight line fitted to the data points for $\ln(\beta/T_p^2)$ versus $1/T_p$ yields the activation energy of the oxidation reaction. This relation is based on first order reaction kinetics, hence:

$$k = A\exp\left(\frac{-E_A}{RT}\right), \quad (2)$$

where k is the reaction rate and A the frequency factor. Earlier studies [31] have shown that a reaction rate, ln$k$, corresponding to -13 generally leads to full healing of cracks of micron sized width within a time span of 1 h, whereas a value of -15 requires 10 h.

2.3. Initiation of local crack damage

As a result of the large differences in hardness and toughness different methods had to be applied to the three materials selected to induce local cracks whose healing behaviour could be studied under the combustion chamber conditions.

In the case of the alumina–TiC composite material Vickers indentation (Zwick/Z2.5, Germany) at a load of 20 N were used to induce penny-shaped cracks. The relationship between the applied load and the length of crack generated was investigated; see figure 1. The indent size ($2a$) is defined by the average of the diagonals of the imprint made, whiles the crack length ($2c$) is defined as the average of the horizontal and vertical cracks formed in addition to the indent size. The fracture toughness was calculated to be 4.3 ± 0.1 MPa m$^{-1/2}$ [32]. This is slightly higher than the reported values for the constituents, i.e., 4.0 ± 0.1 MPa m$^{-1/2}$ for monolithic Al_2O_3 [33] and 3.8 MPa m$^{-1/2}$ for TiC [34]. When applying a load of less than 5 N the Vickers indenter did not generate any crack. However, at 20 N an appreciable surface crack of length 100 μm forms. The cracks opened up to a width of about 1 μm, see figures 5(a) and (b).

In the case of Ti_2AlC samples neither indentation nor an impact method resulted in finite cracks within the samples. In this case thermal shock treatments were applied. Crack formation due to thermal shock first occurred at a temperature difference between heating and cooling of 450 °C. Microcracks of less than 2 μm in width were formed. For maximum temperatures between 450 °C and 950 °C cracks between 5 and 20 mm in length were formed by quenching in water. Based on 16 experiments the results were reproducible. Crack widths remained between 1 and 15 μm in this temperature range

The Ti_2AlC samples used in the combustion study were quenched from 850 °C. This led to a large crack of 10 μm width and 20 mm length in the pure Ti_2AlC disk through the sample thickness. The second Ti_2AlC sample, containing TiC, Ti_3AlC and Ti_3Al impurities formed a crack of 5 μm in width and of approx. 0.5 mm in depth.

In the fine grained Cr_2AlC samples microcracks could be created with the Vickers indenter by applying a load of 300 N for 12 s. Cracks of about 140 μm, having a width of less than 1 μm were obtained. Per disc 10 of such cracks were produced in the samples to be tested in the combustion chamber. The fracture toughness value was estimated to be 8.7 MPa m$^{-1/2}$ using the load dependence of the indentation crack length.

In the case of the coarse grained material indention loading did not result in radial cracks and only caused local plastic deformation. To induce local cracks of finite dimensions, coarse grained Cr_2AlC discs were clamped to a steel plate and subjected to low velocity perpendicular impact using 10 mm tungsten carbide balls. Beyond a critical impact energy, cracks were initiated at the crater edge and then propagated in the radial direction [35–37]. The correlation between impact energy and inducing cracks is depicted in figure 2. The threshold impact energy for Cr_2AlC is about 50 mJ. A crack with a length of 700 μm and a maximum

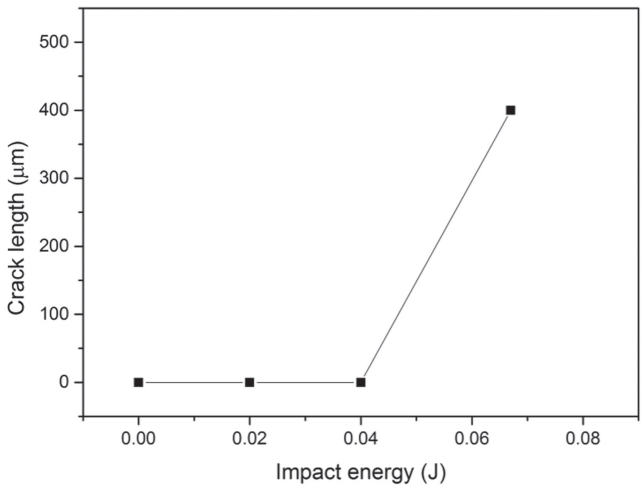

Figure 2. Crack length versus impact energy for cracks created in coarse grained Cr_2AlC by impact of WC balls.

crack opening of 2.5 μm is observed in the coarse grained sample tested in the combustion chamber.

Samples tested in the combustion chamber contained cracks initiated by methods described above. Al_2O_3/TiC composites and both the fine and course grained Cr_2AlC had more than 5 cracks with lengths up to 1 mm and an average width of less than 2 μm. The through crack produced by thermal shock in the high purity Ti_2AlC sample was 10 μm wide and 20 mm in length, while the impurities of the second Ti_2AlC sample resulted in a thinner 5 μm crack with of approx. depth of 0.5 mm, while comparable in length.

2.4. Crack healing in combustion chamber

To investigate healing of crack damage at conditions encountered in a real combustion chamber, samples were placed in a combustor setup (Limousine Combustor, UTwente, The Netherlands [38]); see figure 3. The flow in the combustor is turbulent, as the Reynolds number is well above 4000 for all conditions. The combustor is operated at atmospheric pressure and the gases are injected at room temperature. The fuel used is 100% methane at room temperature. The air and fuel flow are controlled from a PC with control software and mass flow controller valves. The air and fuel mass flow are about 24.62 g s^{-1} and 0.8 g s^{-1}, respectively resulting in an average gas flow speed of 16 m s^{-1} at the location of the samples. The combustor is operated at an operating point with a thermal power of 40 kW and an air excess factor of 1.8. The air factor is the ratio of the actual

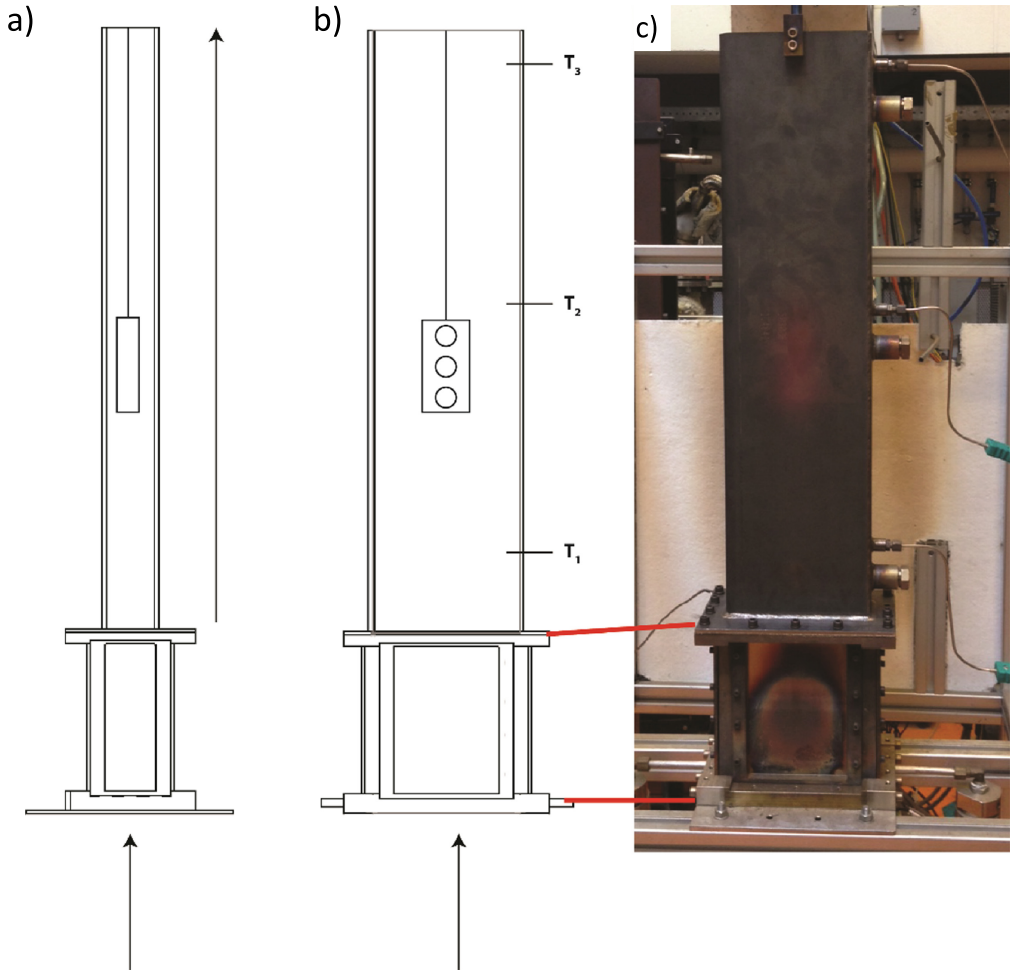

Figure 3. Combustion setup: (a) schematic side view with arrows indicating gas flow direction, (b) front view showing the position of the sample holder and thermocouples and (c) actual experimental setup.

fuel-to-air flow rate ratio to the fuel-to-air flow rate ratio necessary for stoichiometric combustion and indicates the excess of air in the chemical reaction. The combustor can operate in a stable or unstable regime. In the unstable regime pressure oscillations are amplified by the combustion process and they grow in a limit cycle to amplitudes of 160 dB sound pressure level. This phenomenon can happen in gas turbine engines but is to be avoided with a view to fatigue damage. Under the conditions mentioned before, the combustor is running stable and the observed pressure oscillations are lower (about 100 dB) and representative for normal operation of a gas turbine engine. The adiabatic flame temperature and oxygen concentration at equilibrium conditions can be estimated using Chemkin Equil [39] assuming constant pressure and enthalpy. Using the GRI-Mech 3.0 reaction mechanism [40] and an initial temperature of 295 K the adiabatic flame temperature at these operating conditions is estimated to be about 1581 K. Under the above mentioned assumptions of adiabatic, isobaric conditions and assuming that the reacting mixture has already reached the equilibrium state, the oxygen mole fraction at the sample holder location is computed to be about 0.0876. Assuming a mixture of ideal gases, the volume fraction of oxygen then becomes 8.76%vol.

The 6 samples (3 sets of 2) were mounted in an Inconel 800 holder suspended midway in the exhaust of the combustor; see figure 3. Samples are arranged back to back so both samples of one material are exposed to the same conditions; see figure 3(b). After exposure to the chamber conditions for 4.5 h, the samples were removed after switching off the fuel supply and allowing the chamber to cool down in approximately 45 min. The temperature at the sample holder was approx. 1000 °C. Temperature fluctuations during the course of the experiment were of the order of ±2 °C.

After exposure and subsequent cooling down the samples were examined using SEM and XMA. Both the surface and cross-sections prepared by cutting with a diamond blade were investigated regarding the oxides formed and crack gap volume filled.

3. Results

3.1. Materials characterisation

All sintered materials were found to have a density above 95%; see table 3. The ceramic composite samples (Al_2O_3/TiC) showed traces of WC, an impurity of the TiC powder. Impurities in the MAX phase ceramics stem from incomplete reactions during synthesis. Cr_2AlC was prepared with a fine and course grained microstructure resulting in a different hardness, viz. 6.0 and 3.2 GPa, respectively. The average grain sizes are reported in table 3.

3.2. Oxidation of TiC, Ti_2AlC and Cr_2AlC in air and combustion environments

Differential thermal analysis of the powdered healing agents TiC, Ti_2AlC and Cr_2AlC determined oxidation reaction peaks

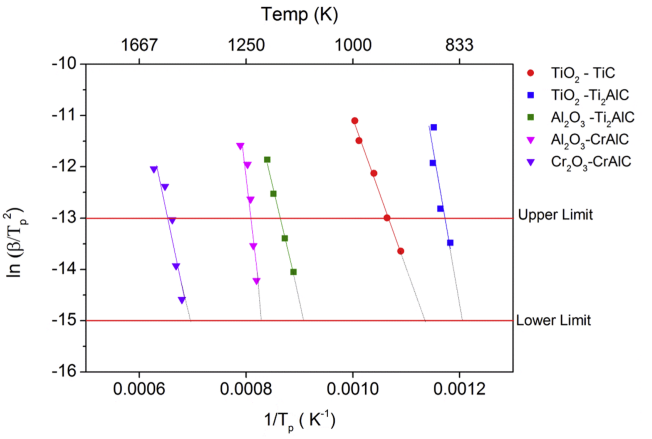

Figure 4. Evaluating the activation energy for the different reactions occurring during oxidation of all healing materials considered (plot of reactivity versus peak temperature).

for all materials below 1300 °C. In figure 4 the reaction rates are plotted as a function of the inverse temperature for the three powders investigated. Taking the values of −15 and −13 for the natural logarithm of the reaction rate as the lower and upper value for optimal healing [31] (see section 2.2), we find the following optimal annealing temperatures, 600 °C–660 °C for the formation of TiO_2 from TiC. For Ti_2AlC the temperature range is 556 °C–580 °C and 826 °C–885 °C for the formation to TiO_2 and Al_2O_3 respectively. And for Cr_2AlC it is 929 °C–963 °C and 1170 °C–1257 °C for the formation of Al_2O_3, and Cr_2O_3 respectively.

After exposure in the combustion chamber for 4 h where the temperature at sample location was measured to be between 940 °C and 1110 °C the colour of the Al_2O_3/TiC samples had changed from very dark grey to light grey, indicating full oxidation. Observations at higher resolution in the SEM showed that islands of TiO_2 formed all over the surface on top of the TiC particles. The activation energy of the complete transformation of TiC to rutile amounts to 242 ± 11 kJ mol^{-1} according to DTA. After removing the surface oxides by diamond polishing complete filling of the cracks with oxide was observed; see figures 5(c) and (d). Even, after removing a layer of about 10 μm by diamond polishing, the indentation induced cracks appeared to be fully filled with oxides. This suggests that the cracks running from the surface inside the composite are healed. Moreover, it seems that the oxides grew laterally from the TiC particles along the crack gap, while the oxides on the surface grew locally.

Observation of the tested Ti_2AlC samples showed dark discoloration on the surface exposed to the combustion environment. Both Ti_2AlC samples showed significant oxide growth after being exposed to the combustion environment for 4 h. Grains of less than 5 μm cover the complete surface and all cracks smaller than 10 μm in width within the indents; see figure 6. The outer layer of the oxide was identified as TiO_2 by SEM–XMA and XRD. A uniform and dense mixed oxide layer with a thickness of about 13 μm developed on the high purity Ti_2AlC material. According to DTA analysis

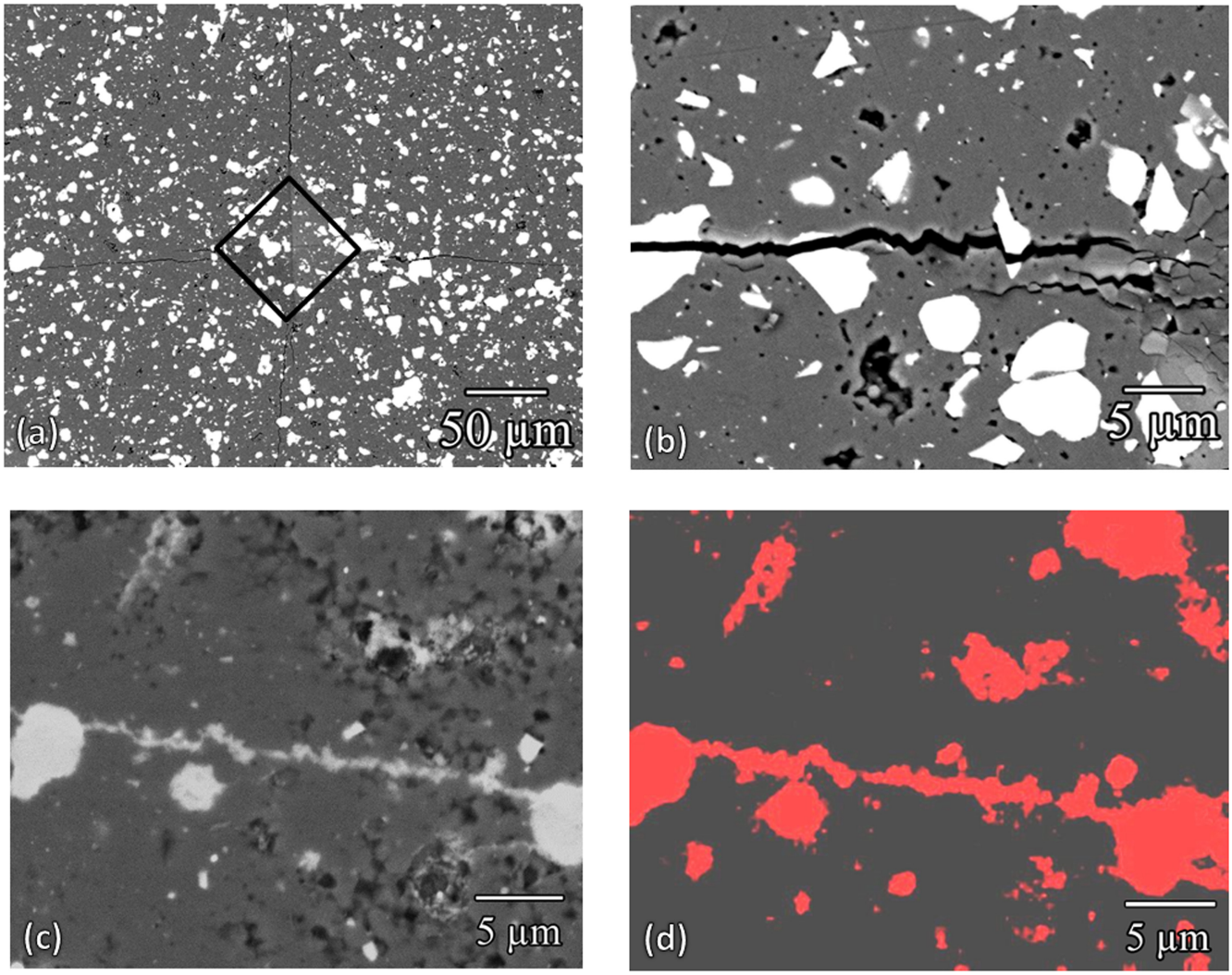

Figure 5. SEM micrographs of Al_2O_3/TiC composite. (a) Cracks created by Vickers indentation: (b) close-up showing crack-particle interaction, (c) healed crack after exposure to combustion environment for 4 h, (d) Ti x-ray mapping showing the filling of the healed crack.

Table 3. Properties of sintered materials and impurities as detected by x-ray diffraction.

Sample	Impurities	Average grain size (μm)	Density (%)	Hardness (GPa)
Al_2O_3/TiC_01	WC	4.5	95%	18.7
Al_2O_3/TiC_02	WC	4.5	99%	19.3
Ti_2AlC-P	none	15–40	95.8%	3.9
Ti_2AlC-LP	TiC, Ti_3AlC_2, TiAl	15–40	95.1%	3.5
Cr_2AlC_FG	Cr	2	99.1%	6.0
Cr_2AlC_CG	Cr_7C_3	20–30	98.7%	3.2

small amounts of TiO_2 are expected to form around 570 °C while full rutile transformation is achieved at 700 °C, followed by Al_2O_3 formation around 800 °C.

The thermally induced crack in pure Ti_2AlC was fully filled with TiO_2 and Al_2O_3 up to a depth of 1.2 mm; see figure 6. Beyond this depth, oxides were formed at the opposing fracture surfaces, however not fully bridging the crack gap. The Ti_2AlC material containing impurities of TiC, Ti_3AlC and Ti_3Al formed a 15 μm thick mixed oxide scale with an outer layer of TiO_2 of approx. 3 μm thickness. The crack, having a jagged path and a width of only 1 μm was fully filled up to its crack tip at a depth of 0.5 mm. The oxide within the crack gap is Al_2O_3. Given that oxidation still occurs at oxygen potentials lower than in atmospheric air (0.088 versus 0.2 atm), the fact that cracks 1.2 mm below the surface were not fully closed was attributed to regions of the crack being sealed by surrounding oxide bridges or to the lower rate of oxidation.

The oxidation of Cr_2AlC requires higher temperatures and is slower compared to Ti_2AlC. Formation of Al_2O_3 begins

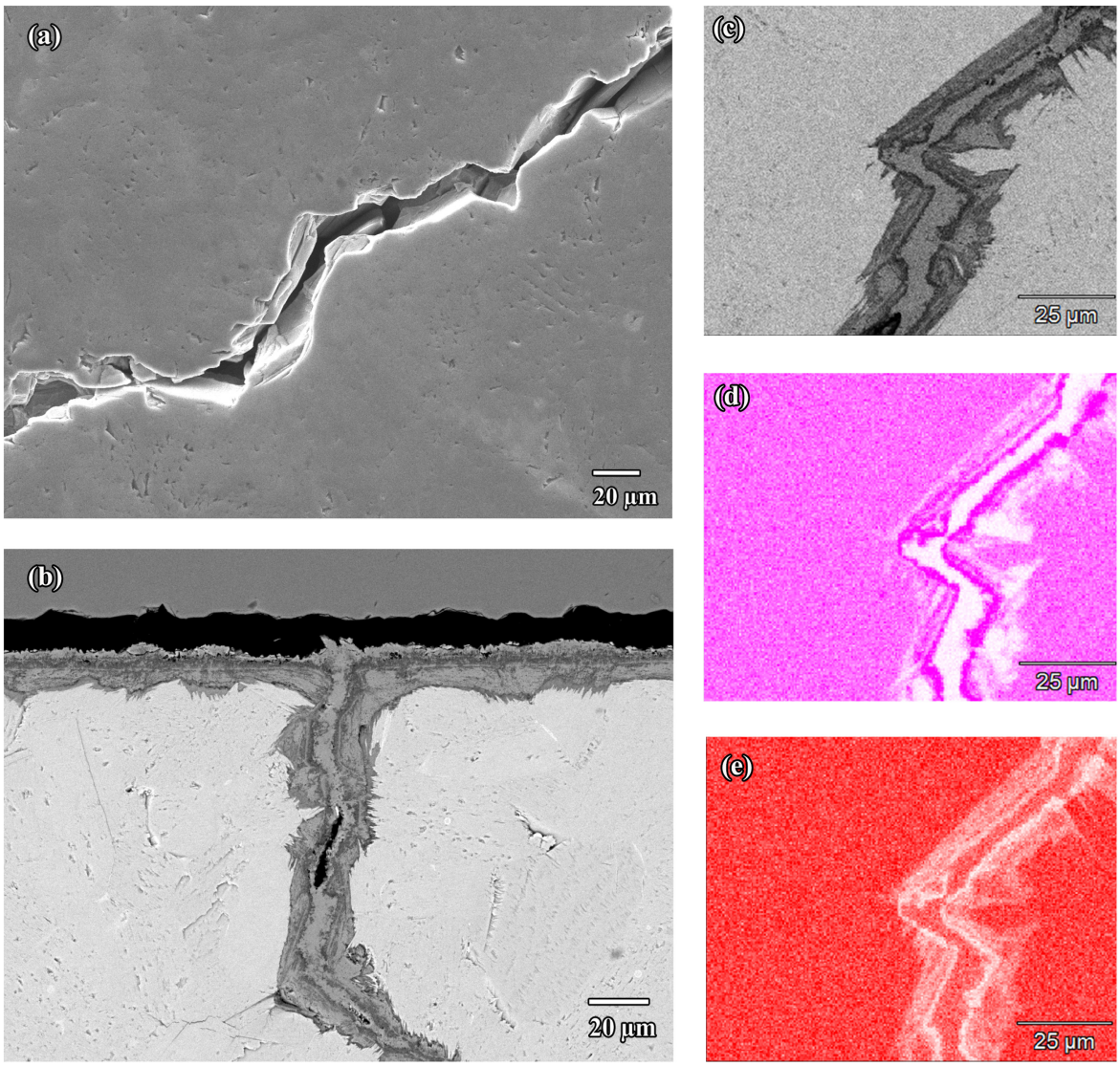

Figure 6. (a) Cracks in Ti_2AlC-A after quenching in water from 850 °C; (b) cross-section of healed crack after exposure to combustion conditions for 4 h; (c) close up of healed crack; (d) Al x-ray map; (e) Ti x-ray map.

around 900 °C to 1000 °C. A second peak in the heat flow signal of the DTA analysis at 1170°–1275° corresponds to the formation of an Al_2O_3 and $(Cr, Al)_2O_3$ solid solution according to XRD. The oxide grown on the surface after 4 h of oxidation in the combustion chamber was about 0.24 μm and 0.19 μm thick on the fine and coarse gained sample, respectively. These oxide layers are thinner than the oxide layers formed in synthetic air for corresponding temperature and time, namely: 0.6 μm and 0.5 μm, respectively. Apparently the lower oxygen partial pressure in the combustion ambient as compared with that of air resulted in low oxide nucleation density (i.e. larger oxide grain size) and consequently slower oxidation kinetics. Hence, cracks with a width of less than 0.5 μm were fully healed with oxide and those with larger crack opening were only partially healed; see figure 7.

The significant difference in oxygen partial pressure from standard self-healing investigations performed in synthetic or atmospheric air (0.2 atm) to the conditions found in the combustion setup (0.088 atm) show no significant impairment of the healing ability in the case of the three tested materials. The lower pO_2 resulted in thinner oxide scales for Cr_2AlC than those found in thermal gravimetric analysis, 0.2–0.5 μm for fine grained Cr_2AlC. Healing in Ti_2AlC and Al_2O_3/TiC was not affected by the reduced oxygen partial pressure. Surprisingly other compositional changes to the atmosphere due to combustions, e.g. higher NO_x content, showed no effect on sample composition.

4. Conclusions

Three high temperature ceramic systems, Al_2O_3/TiC, Ti_2AlC and Cr_2AlC were investigated concerning their fracture, oxidation and self-healing behaviour under real combustion conditions. All tested materials showed full crack-gap filling for 0.5 to more than 10 μm wide cracks of up to 20 mm length, after exposure to the high velocity exhaust gas mixture at approx. 1000 °C for 4 h. Although the oxygen partial

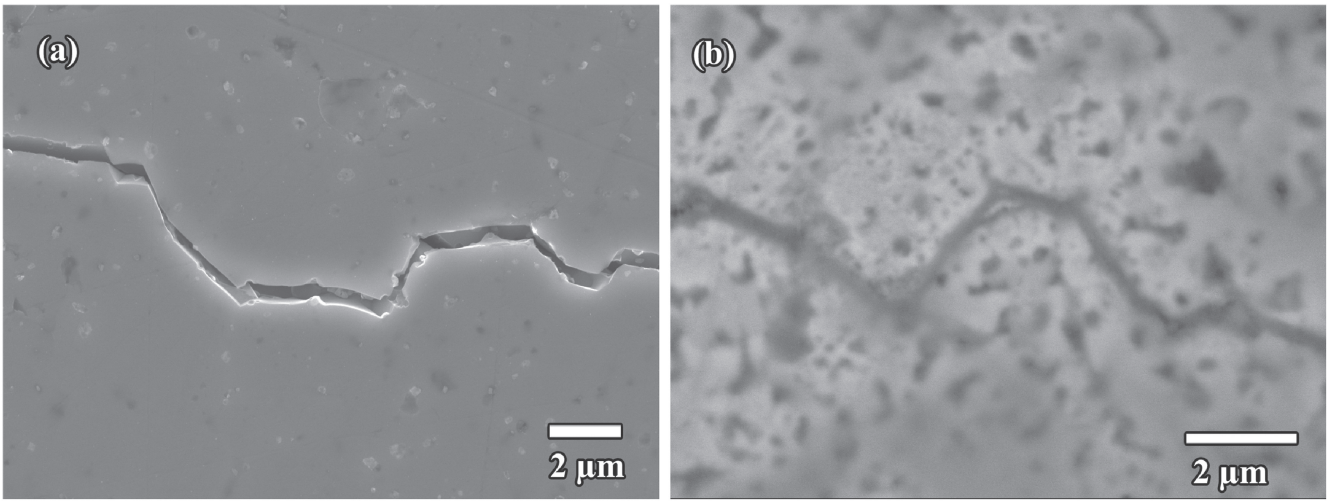

Figure 7. (a) Crack damage in fine grained Cr_2AlC generated by Vickers indentation; (b) crack healed by Al_2O_3 formed in combustion environment for 4 h.

pressure in the combustion chamber is much lower than in air (0.088 versus 0.2 atm), the conditions are sufficient to realise full healing of crack damage. The high gas flow rate (16 m s^{-1}) and thermal load did not impair the healing process.

Acknowledgments

This research was sponsored in part by the People Program (Marie Curie ITN) of the European Union's seventh framework program, FP7, grant number 290308 (SHeMat) and the German Research Foundation (Deutsche Forschungsgemeinschaft, DFG, SPP 1568 'Design and Generic Principles of Self-Healing Materials', under contract SL184/1-2).

References

[1] Song G M, Schnabel V, Kwakernaak C, Van Der Zwaag S, Schneider J M and Sloof W G 2012 High temperature oxidation behaviour of Ti_2AlC ceramic at 1200 °C *Mater. High Temp.* **29** 205–9

[2] Ganguly A, Barsoum M W and Doherty R D 2007 Interdiffusion between Ti_3SiC_2–Ti_3GeC_2 and Ti_2AlC–Nb_2AlC diffusion couples *J. Am. Ceram. Soc.* **90** 2200–4

[3] Li S, Song G, Kwakernaak K, van der Zwaag S and Sloof W G 2012 Multiple crack healing of a Ti_2AlC ceramic *J. Eur. Ceram. Soc.* **32** 1813–20

[4] Ando K, Ikeda T, Sato S, Yao F and Kobayasi Y 1998 A preliminary study on crack healing behaviour of Si_3N_4/SiC composite ceramics *Fatigue Fract. Eng. Mater. Struct.* **21** 119–22

[5] Ando K, Chu M C, Yao F and Sato S 1999 Fatigue strength of crack-healed Si_3N_4/SiC composite ceramics *Fatigue Fract. Eng. Mater. Struct.* **22** 897–903

[6] Kim B S, Ando K, Chu M C and Saito S 2003 Crack-healing behavior of monolithic alumina and strength of crack-healed member *Zairyo* **52** 667–73

[7] Ando K, Chu M-C, Tsuji K, Hirasawa T, Kobayashi Y and Sato S 2002 Crack healing behaviour and high-temperature strength of mullite/SiC composite ceramics *J. Eur. Ceram. Soc.* **22** 1313–9

[8] Takahashi K, Yokouchi M, Lee S-K and Ando K 2003 Crack-healing behavior of Al_2O_3 toughened by SiC whiskers *J. Am. Ceram. Soc.* **86** 2143–7

[9] Osada T, Nakao W, Takahashi K, Ando K and Saito S 2007 Strength recovery behavior of machined Al_2O_3/SiC nano-composite ceramics by crack-healing *J. Eur. Ceram. Soc.* **27** 3261–7

[10] Sugiyama R, Yamane K, Nakao W, Takahashi K and Ando K 2008 Effect of difference in crack-healing ability on fatigue behavior of alumina/silicon carbide composites *J. Intell. Mater. Syst. Struct.* **19** 411–5

[11] Yao F, Ando K, Chu M C and Sato S 2000 Crack-healing behavior, high temperature and fatigue strength of SiC-reinforced silicon nitride composite *J. Mater. Sci. Lett.* **19** 1081–3

[12] Korouš J, Chu M C, Nakatani M and Ando K 2000 Crack healing behavior of silicon carbide ceramics *J. Am. Ceram. Soc.* **83** 2788–92

[13] Yao F, Ando K, Chu M C and Sato S 2001 Static and cyclic fatigue behaviour of crack-healed Si_3N_4/SiC composite ceramics *J. Eur. Ceram. Soc.* **21** 991–7

[14] Ando K, Tuji K, Furusawa K, Hanagata T, Chu M C and Sato S 2001 Effect of pre-crack size and testing temperature on fatigue strength properties of crack healed mullite *Zairyo* **50** 920–5

[15] Yoshioka S, Boatemaa L, Van der Zwaag S, Nakao W and Sloof W G On the use of TiC as high-temperature healing particles in alumina based composites *J. Eur. Ceram. Soc.* in press

[16] Song G M, Pei Y T, Sloof W G, Li S B, De Hosson J T M and van der Zwaag S 2008 Oxidation-induced crack healing in Ti_3AlC_2 ceramics *Scr. Mater.* **58** 13–6

[17] Sloof W G, Li S, Song G, Kwakernaak C, Wu X and Van der Zwaag S 2011 Multiple crack-healing and strenght recovery in MAX phase ceramics *ICSHM 2011: Proc. 3rd Int. Conf. on Self-Healing Materials (Bath, UK, 27–29 June 2011)*

[18] Yang H J, Pei Y T, Rao J C, De Hosson J T M, Li S B and Song G M 2011 High temperature healing of Ti_2AlC: on the origin of inhomogeneous oxide scale *Scr. Mater.* **65** 135–8

[19] Li S, Xiao L, Song G, Wu X, Sloof W G and Van Der Zwaag S 2013 Oxidation and crack healing behavior of a fine-grained Cr_2AlC ceramic *J. Am. Ceram. Soc.* **96** 892–9

[20] Song G M 2012 *Advances in Science and Technology of $M_{n+1}AX_n$ Phases* ed I M Low (Cambridge: Woodhead Publishing) pp 271–88
[21] Tallman D J, Anasori B and Barsoum M W 2013 A critical review of the oxidation of Ti_2AlC, Ti_3AlC_2 and Cr_2AlC in air *Mater. Res. Lett.* **1** 115–25
[22] Farle A-S, Kwakernaak C, van der Zwaag S and Sloof W G 2015 A conceptual study into the potential of $M_{n+1}AX_n$-phase ceramics for self-healing of crack damage *J. Eur. Ceram. Soc.* **35** 37–45
[23] Li S, Chen X, Zhou Y and Song G 2013 Influence of grain size on high temperature oxidation behavior of Cr_2AlC ceramics *Ceram. Int.* **39** 2715–21
[24] Wang J, Zhou Y, Liao T, Zhang J and Lin Z 2008 A first-principles investigation of the phase stability of Ti_2AlC with Al vacancies *Scr. Mater.* **58** 227–30
[25] Liao T, Wang J, Li M and Zhou Y 2009 First-principles study of oxygen incorporation and migration mechanisms in Ti_2AlC *J. Mater. Res.* **24** 3190–6
[26] Barsoum M W and Radovic M 2011 *Annual Review of Materials Research* vol 41 ed D R Clarke and P Fratzl (Palo Alto: Annual Reviews), pp 195–227
[27] Sun Z M 2011 Progress in research and development on MAX phases: a family of layered ternary compounds *Int. Mater. Rev.* **56** 143–66
[28] Duan X, Shen L, Jia D, Zhou Y, van der Zwaag S and Sloof W G 2015 Synthesis of high-purity, isotropic or textured Cr_2AlC bulk ceramics by spark plasma sintering of pressure-less sintered powders *J. Eur. Ceram. Soc.* **35** 1393–400
[29] ASTM B311-93 1997 *Test Method for Density Determination for Powder Metallurgy (P/M) Materials Containing Less Than Two Percent Porosity* (International A)
[30] Kissinger H E 1956 Variation of peak temperature with heating rate in differential thermal analysis *J. Res. Natl Bur. Stand.* **57** 217–21
[31] Yoshioka S and Nakao W 2015 Methodology for evaluating self-healing agent of structural ceramics *J. Intell. Mater. Syst. Struct.* **6** 1395–403
[32] Evans A G and Charles E A 1976 Fracture toughness determinations by indentation *J. Am. Ceram. Soc.* **59** 371–2
[33] Sglavo V M, Trentini E and Boniecki M 1999 Fracture toughness of high-purity alumina at room and elevated temperature *J. Mater. Sci. Lett.* **18** 1127–30
[34] Chermant J L, Deschanvres A and Osterstock F 1978 Toughness and fractography of TiC and WC *Fract. Mech. Ceram.* **4** 891–901
[35] Duó P, Liu J, Dini D, Golshan M and Korsunsky A M 2007 Evaluation and analysis of residual stresses due to foreign object damage *Mech. Mater.* **39** 199–211
[36] Evans A G, Gulden M E and Rosenblatt M 1978 Impact damage in brittle materials in the elastic-plastic response regime *Proc. R. Soc.* A **361** 343–65
[37] Peters J O and Ritchie R O 2000 Influence of foreign-object damage on crack initiation and early crack growth during high-cycle fatigue of Ti–6Al–4V *Eng. Fract. Mech.* **67** 193–207
[38] Roman Casado J C 2013 Nonlinear behavior of the thermoacoustic instabilities in the limousine combustor *PhD Thesis* University of Twente p 156
[39] Kee R, Rupley F, Miller J, Coltrin M, Grcar J, Meeks E, Moffat H, Lutz A, Dixon-Lewis G and Smooke M 2000 *CHEMKIN Collection, Release 3.6* (San Diego, CA: Reaction Design Inc.)
[40] Smith G P *et al* 1999 GRI-Mech 3.0 University of California, Stanford Univerisity and SRI International available from: (http://me.berkeley.edu/gri_mech) **51** p 55